Fully automated segmentation of the right ventricle in patients with repaired Tetralogy of Fallot using U-Net

Tran, Christopher, Halicek, Martin, Dormer, James, Tandon, Animesh, Hussain, Tarique, et al.

Christopher T. Tran, Martin Halicek, James D. Dormer, Animesh Tandon, Tarique Hussain, Baowei Fei, "Fully automated segmentation of the right ventricle in patients with repaired Tetralogy of Fallot using U-Net," Proc. SPIE 11317, Medical Imaging 2020: Biomedical Applications in Molecular, Structural, and Functional Imaging, 113171M (28 February 2020); doi: 10.1117/12.2549052

SPIE.

Event: SPIE Medical Imaging, 2020, Houston, Texas, United States

Fully automated segmentation of the right ventricle in patients with repaired Tetralogy of Fallot using U-Net

Christopher T. Tran [1], Martin Halicek [1,2], James D. Dormer [2], Animesh Tandon [4,5], Tarique Hussain [4,5], Baowei Fei [1,3,4] *

[1] *University of Texas at Dallas, Department of Bioengineering, Richardson, TX, USA*
[2] *Georgia Inst. of Tech. and Emory Univ., Dept. of Biomedical Engineering, Atlanta, GA*
[3] *Advanced Imaging Research Center, Univ. of Texas Southwestern Medical Center, Dallas, TX*
[4] *Dept. of Radiology, Univ. of Texas Southwestern Medical Center, Dallas, TX*
[5] *Department of Pediatrics, Univ. of Texas Southwestern Medical Center, Dallas, TX*

ABSTRACT

Cardiac magnetic resonance (CMR) imaging is considered the standard imaging modality for volumetric analysis of the right ventricle (RV), an especially important practice in the evaluation of heart structure and function in patients with repaired Tetralogy of Fallot (rTOF). In clinical practice, however, this requires time-consuming manual delineation of the RV endocardium in multiple 2-dimensional (2D) slices at multiple phases of the cardiac cycle. In this work, we employed a U-Net based 2D convolutional neural network (CNN) classifier in the fully automatic segmentation of the RV blood pool. Our dataset was comprised of 5,729 short-axis cine CMR slices taken from 100 individuals with rTOF. Training of our CNN model was performed on images from 50 individuals while validation was performed on images from 10 individuals. Segmentation results were evaluated by Dice similarity coefficient (DSC) and Hausdorff distance (HD). Use of the CNN model on our testing group of 40 individuals yielded a median DSC of 90% and a median 95th percentile HD of 5.1 mm, demonstrating good performance in these metrics when compared to literature results. Our preliminary results suggest that our deep learning-based method can be effective in automating RV segmentation.

Keywords: Tetralogy of Fallot, Cardiac magnetic resonance imaging, Deep learning, Convolutional neural network (CNN), Image segmentation, Heart, Left ventricle

1. INTRODUCTION

Tetralogy of Fallot (rTOF) is a congenital heart defect that occurs in about 1 in 2,518 babies born in the United States, and is the most common cyanotic congenital heart disease.[1] Following surgical repair of the condition, patients commonly suffer from pulmonary regurgitation, which can contribute to significant enlargement of the right ventricle (RV), making regular postoperative assessment crucial in curtailing the development of major adverse cardiovascular events.[2]

Cardiac magnetic resonance imaging (CMR) is an imaging modality that is particularly well-suited for evaluation of repaired Tetralogy of Fallot, providing clear images that allow accurate and reproducible measurement of RV size and ejection fraction (EF) to quantify ventricular function.[3] These measures are especially important, as severe ventricular dilation and dysfunction have been found to be useful factors in outcome prediction for patients with rTOF.[4] Unfortunately, taking these measurements in clinical practice can be time-consuming, requiring manual tracing of the endocardium across multiple phases of the cardiac cycle.[5]

Convolutional neural networks (CNNs) are a class of deep learning algorithms. The U-Net architecture has been shown to be especially useful in the localization of structures in biomedical images.[6] Using a U-Net based CNN to perform this simple but tedious delineation task has the potential to save the time for clinicians who perform the current labor-intensive standard of practice. The objective of this study is to investigate the feasibility of CNN-based automatic segmentation of the RV endocardium on short-axis cine CMR images of patients with rTOF.

* E-mail: bfei@utdallas.edu ; Web: www.fei-lab.org

Medical Imaging 2020: Biomedical Applications in Molecular, Structural, and Functional Imaging, edited by Andrzej Krol, Barjor S. Gimi, Proc. of SPIE Vol. 11317, 113171M · © 2020 SPIE · CCC code: 1605-7422/20/$21 · doi: 10.1117/12.2549052

2. METHODS

2.1 Tetralogy of Fallot dataset

This study included images with a resolution of 256×256 pixels from 100 individuals (age, 18.0 ± 8.5 years (range, 7-53 years); 58 males, 42 females) with rTOF who had been enrolled in a prospective study between April 2005 and March 2008 across 14 centers participating in the German Competence Network for Congenital Heart Disease. Short-axis images of the heart for volumetric analysis were obtained via a balanced steady-state free-precession gradient-echo sequence with retrospective ECG gating. The standardized CMR protocol used within the network has been described in more detail in previously published works.[7] The dataset was divided randomly into groups for training (N= 50; including 2,958 images), validation (N=10; including 480 images), and testing (N=40; including 2,291 images). One patient in the training data had previously received a pulmonary valve replacement, resulting in metal-induced artifacts near the region of interest for those images.

Delineation of the RV endocardium was performed by cardiologists on images of the heart at end-diastole (ED) and end-systole (ES), as well as on a number of images that correspond to time points between ED and ES. After manual annotation, a total of 5,729 unique images were available for use with the 2D-CNN classifier based on U-Net in MATLAB 2019a (MathWorks Inc., Natick, MA). Pixel intensities for each image were normalized to a range of [0,1].

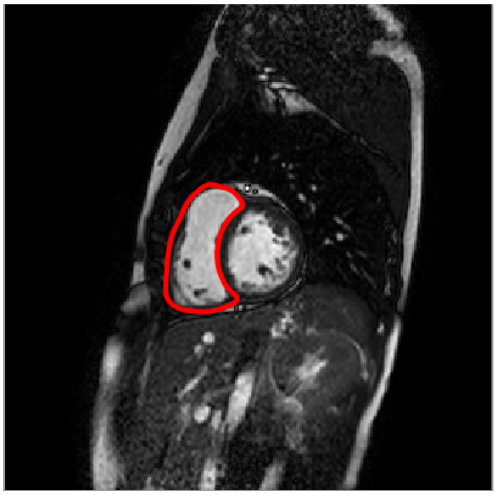

Figure 1. Example cardiologist annotated RV endocardium contour on short-axis cine CMR.

2.2 Convolutional neural network

The U-Net architecture consists of a contracting path, a bottleneck, and an expansion path. The contracting path is composed of several blocks, each of which apply two 3×3 convolutional layers followed by a 2×2 max pooling layer. Each contraction block in the path will output to the next, doubling the number of feature maps in the process, until reaching the bottleneck, which mediates between contraction and expansion, applying two 3×3 convolutional layers before a 2×2 up-convolution layer. Each expansion block consists of two 3×3 convolutional layers followed by a 2×2 upsampling layer.

Skip connections concatenate feature maps from contraction blocks to the corresponding expansion blocks to aid in reconstruction of the segmented image. Only pixels in each probability map with values over 0.5 were used to create the final prediction.

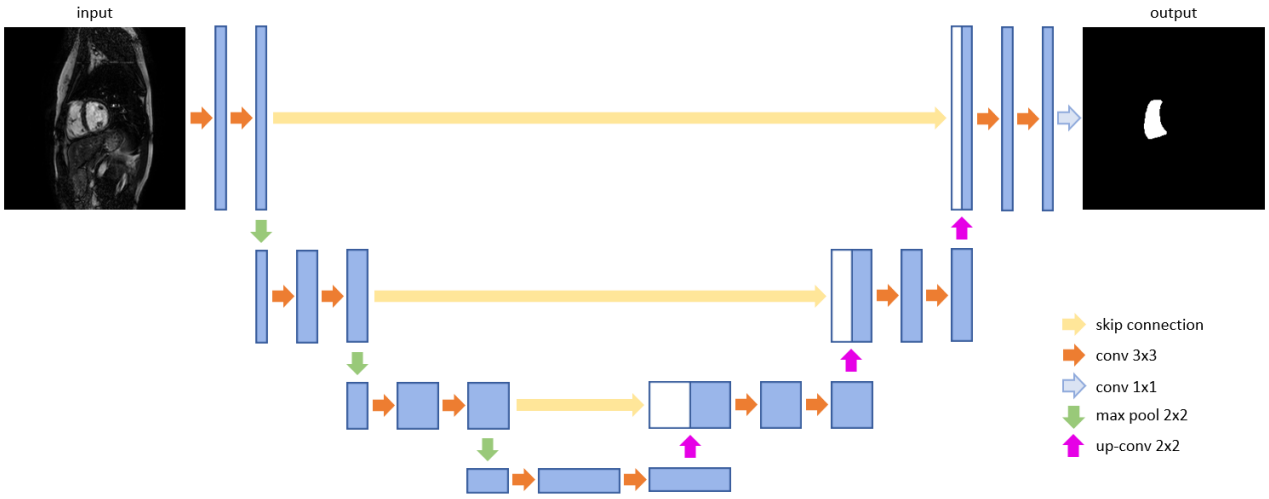

Figure 2. The U-Net architecture for the proposed RV segmentation model.

2.3 Image post-processing

Because each image contains blood pools which do not correspond to the RV, only the largest continuous area predicted by the CNN was evaluated with the aforementioned metrics in order to eliminate false positives. After selection of this area, the prediction mask underwent morphological closing using a disk of a 3-pixel radius as the morphological structuring element.

2.4 Evaluation metrics

Our segmentation results were evaluated primarily using DSC, a measure of overlap between two areas.[8] DSC is given by Equation 1, where M represents the manually drawn contour and P represents the prediction produced by the CNN.

$$DSC = \frac{2|P \cap M|}{|P|+|M|} \tag{1}$$

Additionally, Hausdorff Distance (HD) was calculated as another measure of the CNN's performance. HD is the maximum distance of a set to the nearest point of another set, as given by equation 2, where p and m are the set of points along the perimeters of P and M, respectively, and $d(.,.)$ represents the Euclidean distances from one set of points to the other.[9]

$$HD = \max\{\max_{p \in P} \min_{m \in M} d(p,m), \max_{m \in M} \min_{p \in P} d(m,p)\} \tag{2}$$

3. RESULTS

3.1 Optimal CNN parameters

Our CNN was trained for 18 epochs with the Dice similarity coefficient (DSC) serving as the loss function. Optimal hyperparameters were determined to be a batch size of 12, an encoder depth of 3, and an initial learning rate of 1e-4 with a learning rate drop factor of 0.3 applied every 3 epochs.

3.2 Image categorization

Images were categorized into phases by the areas of their respective manual contours. Within each slice of the short-axis CMR, the contour with the largest area was defined as occurring at ED, the contour with the smallest area was defined as occurring at ES, and the remaining contours were categorized as mid-phase, occurring during either diastole or systole. Images from the superior third of the heart were defined as basal slices, while images from the middle and inferior third were defined as mid-ventricle and apical slices, respectively.

3.3 Final segmentation

An overall median DSC of 0.894 and an overall median 95th percentile HD of 5.5 mm were obtained on the validation dataset of 10 patients using our method. Performance on our testing dataset of 40 patients was comparable, yielding an overall median DSC of 0.898 and an overall median 95th percentile HD of 5.1 mm.

Table 1. Evaluation metrics for RV segmentation on the test group.

		DSC (%)		HD_{95} (mm)	
		Median	Mean ± Std	Median	Mean ± Std
End-Diastole	Basal	91	79 ± 25	5.5	10.1 ± 11.1
	Mid-Ventricle	90	82 ± 21	5.5	8.9 ± 9.0
	Apical	92	84 ± 17	5.1	8.8 ± 9.2
Mid-Phase	Basal	90	80 ± 23	4.9	9.1 ± 10.4
	Mid-Ventricle	91	82 ± 20	4.7	9.0 ± 9.4
	Apical	91	81 ± 23	4.9	8.5 ± 9.0
End-Systole	Basal	87	74 ± 26	5.4	11.9 ± 13.0
	Mid-Ventricle	88	76 ± 27	5.5	9.7 ± 11.1
	Apical	81	71 ± 27	6.2	10.8 ± 9.6
Overall		90	80 ± 23	5.1	9.4 ± 10.1

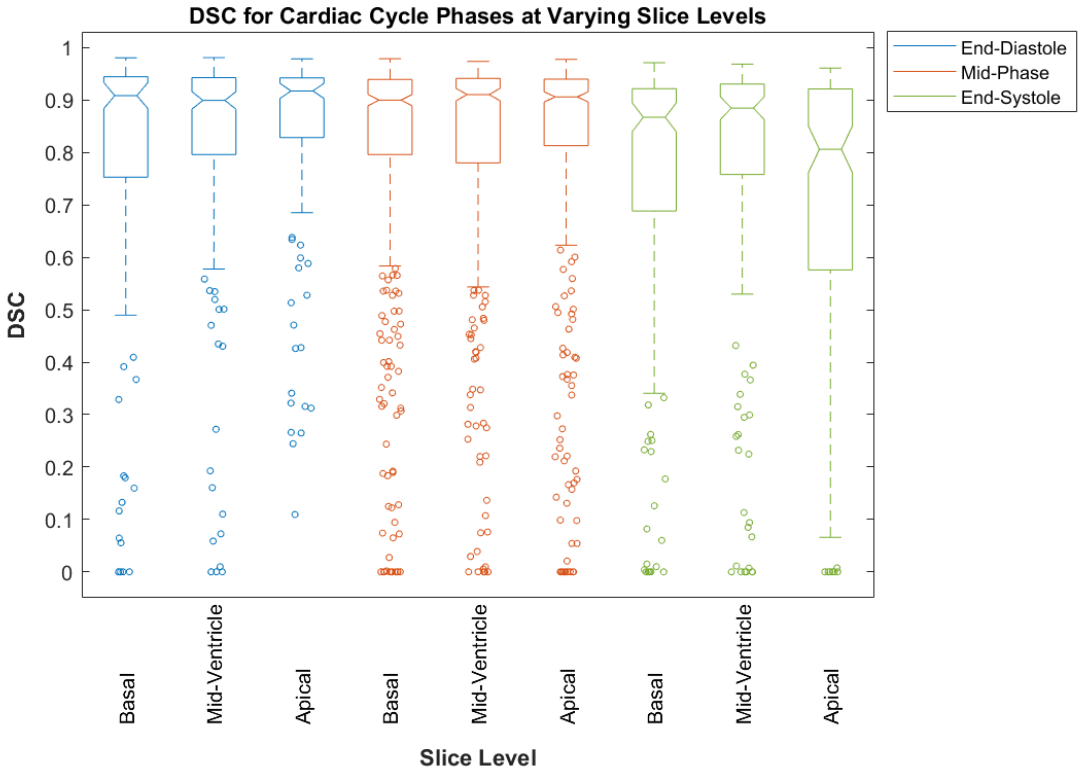

Figure 3. Distribution of DSC results of RV segmentation by the U-Net-based CNN on the test group. Boxplots have been generated for each combination of two categories: cardiac cycle phase (End-Diastole, Mid-Phase, End-Systole) and slice level of the heart (Basal, Mid-Ventricle, Apical).

Our method performs worst on images taken at ES, especially at the apex of the heart. This poor performance at apical ES images may be linked to partial obstruction of the RV blood pool by myocardium as the heart contracts. The presence of the right atrium in basal slices of patients with severe dilation of the RV also appears to present a challenge.

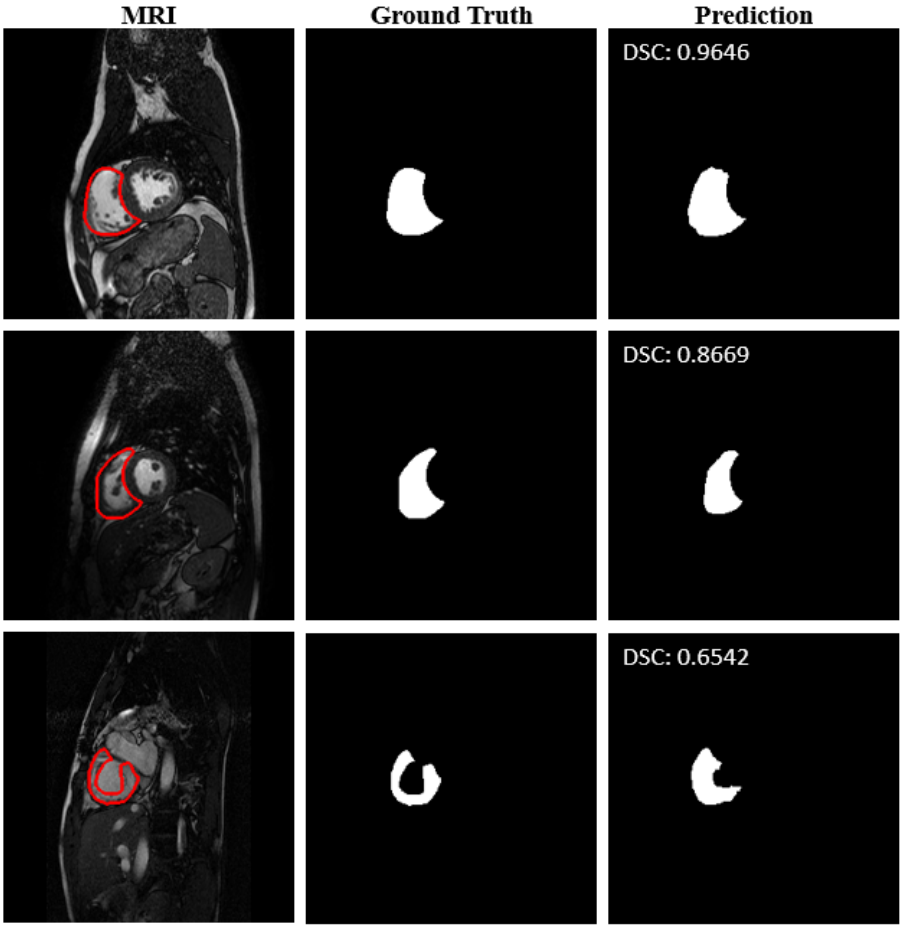

Figure 4. Segmentation results of 3 representative test group patients. Left column: short-axis cine CMR with cardiologist annotation overlaid. Middle column: binary ground truth mask. Right column: CNN prediction.

4. DISCUSSION

In this paper, we evaluated a fully automatic method for RV segmentation of short-axis cine CMR images by a U-Net model. We demonstrated that a single CNN is able to learn useful features for segmenting the RV on images from a diverse patient group. Despite the challenging anatomical and developmental variances in our dataset, we have obtained results comparable to those found in the literature, suggesting that our proposed automatic method is capable of performing this task accurately across different age groups.

While all patients in the dataset display abnormal cardiac anatomy, all suffer from the same condition. The implications of this similitude present a concern that the model may have overfitted to the training pathology. However, the impact of this limitation was most likely mitigated by the large variability in levels of severity among the patients. A dataset containing a variety of healthy and abnormal hearts could produce a more generalizable model.

One other major limitation of this study was the use of only images that were positive for the presence of the RV blood pool. As such, the use of our current method would require the selection of the slices of each CMR that need to be segmented. Future work to improve and further automate this step would explore the introduction of additional networks to discern which CMR slices do or do not contain the RV blood pool in view.

5. CONCLUSION

We developed a deep learning-based method for automatic segmentation of the right ventricle on CMR images. Though the problem of heart chamber segmentation has been tackled a number of times, automatic segmentation of the right ventricle in particular is still a challenge.[10-12] Other studies have approached this problem using similar methods as the one presented, but many share the same dataset of healthy adult patients, and still others use a dataset containing only a few patients.[13-17] Our dataset is unique in not only its larger size, but also its inclusion of children and adolescents as well as adults, all of whom present with cardiac pathology. All of the mentioned factors have been included in this paper to yield a more general and realistic result for RV segmentation, and the confounding factors have been retained in the dataset for objectivity. Nonetheless, the results presented in this paper are comparable with state-of-the-art methods. The CNN-based method may provide a useful tool for clinical applications.

DISCLOSURES

The authors have no relevant financial interests in this article and no potential conflicts of interest to disclose.

ACKNOWLEDGEMENTS

This research was supported in part by the U.S. National Institutes of Health (NIH) grants R01HL140325, R01CA156775, R01CA204254, and R21CA231911) and by the Cancer Prevention and Research Institute of Texas (CPRIT) grant RP190588.

REFERENCES

[1] Centers for Disease Control and Prevention, “Tetralogy of Fallot" (2018).

[2] Ammash, N. M., Dearani, J. A., Burkhart, H.M., and Connolly, H.M., “Pulmonary regurgitation after tetralogy of Fallot repair: clinical features, sequelae, and timing of pulmonary valve replacement.” Congenital Heart Disease, 2(6), 386-403 (2007).

[3] Valente, A. M., and Geva, T., “How to Image Repaired Tetralogy of Fallot,” Circulation: Cardiovascular Imaging, 10(5), e004270 (2017).

[4] Knauth, A.L., Gauvreau, K., Powell, A.J., Landzberg, M.J., Walsh, E.P., Lock, J.E., del Nido, P.J., and Geva, T., “Ventricular size and function assessed by cardiac MRI predict major adverse clinical outcomes late after tetralogy of Fallot repair,” Heart, 94(2), 211-216 (2008).

[5] Kilner, P.J., Geva, T., Kaemmerer, H., Trindade, P.T., Schwitter, J., and Webb, G.D., “Recommendations for cardiovascular magnetic resonance in adults with congenital heart disease from the respective working groups of the European Society of Cardiology”, European Heart Journal, 31(7), 794–805 (2010).

[6] Ronneberger, O., Fischer, P., and Brox, T., “U-net: Convolutional networks for biomedical image segmentation,” Medical Image Computing and Computer-Assisted Intervention – MICCAI 2015, 234-241, Springer International Publishing (2015).

[7] Beerbaum, P., Barth, P., Kropf, S., Sarikouch, S., Kelter-Kloepping, A., Franke, D., Gutberlet, M., Kuehne, T., “Cardiac function by MRI in congenital heart disease: impact of consensus training on interinstitutional variance.” Journal of Magnetic Resonance Imaging, 30(5), 956–966 (2009).

[8] Dice, L.R., “Measures of the amount of ecologic association between species,” Ecology, 26(3), 297–302 (1945).

[9] Huttenlocher, D., Klanderman, G., Rucklidge, W., “Comparing images using the Hausdorff distance,” IEEE Transactions on Pattern Analysis and Machine Intelligence, 15(9), 850–863 (1993).

[10] Santiago, C., Nascimento, J.C., Marques, J.S., “Fast segmentation of the left ventricle in cardiac MRI using dynamic programming,” Computer Methods and Programs in Biomedicine, 154, 9-23 (2018).

[11] Nasr-Esfahani, M., Mohrekesh, M., Akbari, M., Soroushmehr, S.M., Nasr-Esfahani, E., Karimi, N., Samavi, S., Najarian, K., “Left ventricle segmentation in cardiac MR images using fully convolutional network,” arXiv preprint arXiv:1802.07778, (2018).

[12] Irshad, M., Sharif, M. Yasmin, M., Khan, A., “A Survey on Left Ventricle Segmentation Techniques in Cardiac Short Axis MRI,” Current Medical Imaging, 14(2), 223-237 (2018).

[13] Petitjean, C., Zuluaga, M.A., Bai, W., Dacher, J.N., Grosgeorge, D., Caudron, J., Ruan, S., Ayed, I.B., Cardoso, M.J., Chen, H.C., Jimenez-Carretero, D., Ledesma-Carbayo, M.J., Davatzikos, C., Doshi, J., Erus, G., Maier, O.M., Nambakhsh, C.M., Ou, Y., Ourselin, S., Peng, C.W., Peters, N.S., Peters, T.M., Rajchl, M., Rueckert, D., Santos, A., Shi, W., Wang, C.W., Wang, H., Yuan, J., "Right ventricle segmentation from cardiac MRI: a collation study," Medical Image Analysis, 19(1), 187–202 (2015).

[14] Dormer, J. D., Guo, R., Shen, M., Jiang, R., Wagner, M.B., Fei, B., "Ultrasound Segmentation of Rat Hearts Using Convolution Neural Networks." Proc. SPIE 10580, 105801A (2018).

[15] Dormer, J.D., Ma, L., Halicek, M., Reilly, C.M., Schreibmann, E., Fei, B., "Heart Chamber Segmentation from CT Using Convolutional Neural Networks." Proc. SPIE 10578, 105782S (2018).

[16] Qin, X., Cong, Z., Fei, B., "Automatic segmentation of right ventricular ultrasound images using sparse matrix transform and a level set." Physics in Medicine and Biology, 58(21), 7609-7624 (2013).

[17[Qin, X., Cong, Z., Halig, L.V., Fei, B., "Automatic Segmentation of Right Ventricle on Ultrasound Images Using Sparse Matrix Transform and Level Set." Proc. SPIE 8669, 86690Q (2013).